

Crizotinib, a c-Met Inhibitor, Prevents Metastasis in a Metastatic Uveal Melanoma Model

Oliver Surriga¹, Vinagolu K. Rajasekhar¹, Grazia Ambrosini¹, Yildirim Dogan², Ruimin Huang³, and Gary K. Schwartz¹

Abstract

Uveal melanoma is the most common primary intraocular malignant tumor in adults and half of the primary tumors will develop fatal metastatic disease to the liver and the lung. Crizotinib, an inhibitor of c-Met, anaplastic lymphoma kinase (ALK), and ROS1, inhibited the phosphorylation of the c-Met receptor but not of ALK or ROS1 in uveal melanoma cells and tumor tissue. Consequently, migration of uveal melanoma cells was suppressed *in vitro* at a concentration associated with the specific inhibition of c-Met phosphorylation. This effect on cell migration could be recapitulated with siRNA specific to c-Met but not to ALK or ROS1. Therefore, we developed a uveal melanoma metastatic mouse model with EGFP-luciferase-labeled uveal melanoma cells transplanted by retro-orbital injections to test the effect of crizotinib on metastasis. In this model, there was development of melanoma within the eye and also metastases to the liver and lung at 7 weeks after the initial transplantation. When mice were treated with crizotinib starting 1 week after the transplantation, we observed a significant reduction in the development of metastases as compared with untreated control sets. These results indicate that the inhibition of c-Met activity alone may be sufficient to strongly inhibit metastasis of uveal melanoma from forming, suggesting crizotinib as a potential adjuvant therapy for patients with primary uveal melanoma who are at high risk for the development of metastatic disease. *Mol Cancer Ther*; 12(12); 2817–26. ©2013 AACR.

Introduction

Uveal melanoma is the most common primary intraocular malignant tumor in adults. Tumor epicenters are usually found in the choroid, but may also arise from the iris and ciliary body. About 45% of uveal melanoma cases were recorded in adults older than 60 years and 53% were in adults ages between 21 and 60 years old (1). The 5-year survival rate of uveal melanoma patients from 1973 to 2008 is 81.6% (2). However, the prognosis is worse for patients that develop metastatic uveal melanoma with an overall 1- to 2-year survival rate of 13% and 8%, respectively (3, 4). About half of patients with uveal melanoma will develop metastasis, which primarily occurs in the liver (5, 6). In fact, nearly all patients with uveal melanoma that die due to metastatic disease have liver metastasis (7). Uveal melanomas are characterized by mutations in the

G-protein genes, *GNAQ* and *GNA11*. Although the loss of chromosome 3 (5, 8) and mutations in the *BAP1* gene are additionally implicated in uveal melanoma metastasis (9, 10), there has been a considerable interest on the possible role of c-Met, which is highly expressed in metastatic uveal melanoma tumors (5, 11).

The receptor tyrosine kinase (RTK), c-Met, is a 140 kDa transmembrane protein consisting of a disulfide-linked heterodimer with an extracellular α -subunit and a transmembrane β -subunit. When c-Met is bound to its ligand, hepatocyte growth factor (HGF), the autophosphorylation of tyrosine residues are initiated at Tyr1230/1234/1235 in the catalytic domain propagating a signaling cascade through a number of adaptor and effector proteins. This signaling results in the activation of the Ras-ERK, STAT, and PI3K-AKT pathways, which are implicated in oncogenic cell proliferation, survival, and motility (12–14). However, a study has shown that the activation of the previously mentioned pathways through c-Met signaling may not be enough to induce mitogenesis in the cells (15). Other RTKs, namely EGF receptor (EGFR), VEGF receptor (VEGFR), and insulin-like growth factor 1 receptor (IGF1R) may work in conjunction with or propagate the activation of c-Met to initiate mitogenic pathways (6, 16, 17). Previous studies have shown that HGF influences migratory ability *in vitro* (18) and its self-expression may contribute to metastasis *in vivo*. Activated c-Met, a result of indirect gene activation rather than mutation, has also been found in uveal melanoma

Authors' Affiliations: ¹Jennifer Goodman Linn Laboratory of New Drug Development, Department of Medicine; Departments of ²Cell Biology; and ³Radiology, Memorial Sloan-Kettering Cancer Center, New York, New York

Note: Supplementary data for this article are available at Molecular Cancer Therapeutics Online (<http://mct.aacrjournals.org/>).

O. Surriga and V.K. Rajasekhar share first authorship for this article.

Corresponding Author: Gary K. Schwartz, Memorial Sloan-Kettering Cancer Center, 1275 York Avenue, New York, NY 10065. Phone: 212-639-8324; Fax: 212-717-3561; E-mail: schwartzg@mskcc.org

doi: 10.1158/1535-7163.MCT-13-0499

©2013 American Association for Cancer Research.

cell lines (19). Furthermore, previous studies have implicated the increased expression of c-Met in primary uveal melanoma tumors with the higher risk of liver metastasis (6, 11).

Crizotinib is a small-molecule inhibitor that is selective for c-Met as well as anaplastic lymphoma kinase (ALK) and (ROS1). It has been shown to inhibit cell proliferation, migration, and invasion of several tumor cell lines *in vitro* and it has also displayed significant antitumor activity in xenograft mouse models (20–22). It is approved for the treatment of ALK expressing advanced and metastatic non-small cell lung cancer. Because the survival rate of uveal melanoma patients decreases as metastatic disease progresses and that previous studies suggest the significant role of c-Met in uveal melanoma metastasis, there may also be a potential for using crizotinib to prevent the development of metastatic uveal melanoma. This study, therefore, investigates the effects of crizotinib in uveal melanoma cell lines and in a metastatic uveal melanoma model.

Materials and Methods

Cell culture and reagents

C918 and Mel290 were received from Robert Folberg in 2009 (University of Illinois, Chicago, IL). Of note, Mel285, Omm1.3, and Omm1 were kindly provided by Boris Bastian in 2010 (Memorial Sloan-Kettering Cancer Center, New York, NY). Of note, 92.1 was obtained from William Harbour in 2009 (Washington University, St. Louis, MO). C918 was derived from a patient tumor by Daniels and colleagues (23). Mel290 and Mel285 were established from primary tumors by Bruce Ksander (Schepens Eye Research Institute, Boston, MA; ref. 24). Note that 92.1 was established from a primary tumor by Marline Jager (Leiden University Medical Center, Leiden, the Netherlands; ref. 25). Omm1.3 was established from liver metastases also by Bruce Ksander (Schepens Eye Research Institute; ref. 26). Omm1 was established from a patient's subcutis metastatic lesion by G.P.M. Luyten (Rotterdam University Hospital, Rotterdam, the Netherlands; ref. 27). Uveal melanoma cell lines have been sequenced for the presence of activating mutations in codons 209 (exon 5) and 183 (exon 4) of *GNAQ* and *GNA11*. Of note, 92.1 and Omm1.3 had *GNAQ* mutation, whereas Omm1 had *GNA11* mutation. A karyotype test was also performed for each cell line in 2012. Cells were cultured in RPMI medium supplemented with 10% FBS, 100 U/mL penicillin, and 100 mg/mL streptomycin and maintained at 37°C in 5% CO₂. Crizotinib, graciously supplied by Pfizer, was dissolved in dimethyl sulfoxide (DMSO) for *in vitro* experiments and formulated in water for animal studies.

ELISA

For each uveal melanoma cell line, 2 million cells were used to seed 60 mm plates in 3 mL volume of serum-free RPMI media in duplicates. Cells were allowed to grow for 24 hours and the media were collected and centrifuged.

The supernatants were used in the R&D Systems Quantikine ELISA Human HGF Immunoassay according to the manufacturer's instructions. Serum-free media from unseeded plates were used to subtract the background. The presence of HGF in the media is expressed as pg/mL concentrations and the minimum detectable dose of the assay is less than 40 pg/mL.

Immunoblotting

Cells and tissues were lysed with radioimmunoprecipitation assay (RIPA) buffer supplemented with protease inhibitor cocktail tablets (Roche Diagnostics) and 1 mmol/L Na₃VO₄. Equal amounts of protein were loaded on 4% to 12% PAGE gels (Invitrogen). Polyvinylidene difluoride membranes were blocked with 5% nonfat dried milk and probed with p-Met (Y1234-1235), Met, p-ALK (Y1096), ALK, p-ROS1 (Y2274), ROS1, p-STAT3 (Y705), STAT3, p-AKT (S473), AKT, p-ERK 1/2 (T202/Y204), ERK 1/2, cleaved PARP, and α -tubulin (Cell Signaling Technology) and human HGF (Santa Cruz Biotechnology).

Gene silencing

Cells were plated on 60-mm plates, and transfected with control, c-Met, ALK, or ROS1 siRNA using Lipofectamine RNAiMAX (Invitrogen) according to the manufacturer's protocol. The transfections were performed twice, each time in overnight incubations with a recovery phase of 6 hours in between transfections. The siRNA sequences for control, c-Met, ALK, and ROS1 were purchased from Cell Signaling Technology.

Cell viability assays

Cells were plated in 96-well plates and treated in triplicates with the indicated concentrations of crizotinib or DMSO. Viability was assessed after 72 hours of treatment using the Cell Counting Kit 8 (CCK8) from Dojindo Molecular Technologies according to the manufacturer's instructions. Survival is expressed as a percentage of untreated cells. For the c-Met siRNA viability assay, cells were harvested after transfection and grown in triplicates in 96-well plates for 72 hours. Viability was assessed as previously described.

Migration assays

Cells were seeded and treated with DMSO, 25 or 250 nmol/L crizotinib for 24 hours in media with 0.1% serum on BioCoat Matrigel Invasion Chambers (BD Biosciences) according to the manufacturer's instructions. RPMI medium with 10% serum and 50 ng/mL HGF was used as chemoattractant. Noninvading cells were then removed from the Matrigel and cells on the other side of the matrix were fixed with 100% methanol and stained with 1% Toluidine Blue. Images of stained cells were taken through a microscope. For the c-Met, ALK, and ROS1 siRNA migration assay, cells were harvested after double transfection and seeded in triplicates on invasion chambers for 24 hours as mentioned above. RPMI medium with 10% serum and no HGF was used as chemoattractant.

Images of stained cells were obtained from three random sections of each Matrigel to account for cell distribution. Invading cells were then quantified by adding cells from the three sections and calculating the mean of each triplicate. Migration is expressed as the number of cells migrated.

Xenograft studies

Of note, 8-week-old nu/nu SCID (severe combined immunodeficient mice) male mice bearing subcutaneously injected Omm1.3 or 92.1 tumors (9 mice/cohort) of approximately 100 mm³ diameter were treated orally with vehicle control (water) or crizotinib (50, 75, and 100 mg/kg/d) 5 days per week for 3 weeks. Tumors were measured every 2 to 3 days with calipers and tumor volumes were calculated and expressed in cubic millimeter and calculated using the formula $p/6 \times (\text{large diameter}) \times (\text{small diameter})$. Toxicity was monitored by weight loss. Two animals from each cohort were sacrificed 1 to 3 hours after the fifth treatment and tumors were collected. Tumor tissues were carefully dissected from the surrounding stroma and were immediately flash-frozen in liquid nitrogen. Frozen tumors were ground in tubes with resin and RIPA buffer following procedures set for the Sample Grinding Kit (GE Healthcare). The Memorial Sloan-Kettering Cancer Center Institutional Animal Care and Use Committee and Research Animal Resource Center specifically approved this study. The study also complied with the principles of Laboratory Animal Care (NIH publication no. 85-23, released 1985). All efforts were made to minimize suffering.

Construct and preparation of recombinant lentivirus

An flap-Ub promoter-GFP-WRE (FUGW)-based lentiviral vector encoding EGFP/luciferase fusion gene (FUGLW) under the ubiquitin promoter was used to infect the uveal melanoma tumor cells. The viral supernatant was prepared by cotransfecting 293T cells with the FUGLW, pCMV-d8.91, and pMD2.G vectors. Viral transduction was performed as previously described by Dogan and colleagues (28).

Metastatic model

Omm1.3 cells were stably infected with a lentiviral construct to constitutively express the GFP-luciferase fusion protein. EGFP-positive cells were then enriched by fluorescence-activated cell sorting. Note that 8-week-old nu/nu SCID male mice were anesthetized with 3% isoflurane and 10 million cells were administered in 50 μ L PBS through retro-orbital injection. One week later, animals were treated orally with vehicle control or 50 mg/kg crizotinib daily 5 days per week for 9 weeks. Luciferase activity was monitored weekly to detect metastasis progression. At the endpoint, livers and lungs were harvested for immunoblotting and immunohistochemistry. Experiments were carried out under institutional guidelines addressing the proper and humane use of animals. The Memorial Sloan-Kettering Cancer Center Institutional Animal Care and Use Committee and Research Animal

Resource Center specifically approved this study. The study also complied with the Principles of Laboratory Animal Care (NIH Publication No. 85-23, released 1985). All efforts were made to minimize suffering.

Bioluminescence imaging *in vivo*

The imaging procedure was performed under 2.5% isoflurane anesthesia. The animals were injected retro-orbitally with potassium D-luciferin (30 mg/kg; Caliper) and imaged immediately after injection using an IVIS 200 imaging system (Caliper). Living Image software (version 4.0) was used to acquire and quantify the absolute bioluminescence intensity (photons/sec). Regions of interest for both metastatic tumors and background were selected from equivalent-sized areas. The background intensity was subtracted from the signal intensities.

Histopathology

For immunohistochemical analysis, representative sections of tumors were deparaffinized, rehydrated in graded alcohols, and subjected to antigen retrieval by microwave oven treatment using standard procedures. Hematoxylin and eosin (H&E) staining was carried out using Gill hematoxylin (Poly Scientific R&D Corp.) for 10 minutes as per the manufacturer's protocol, followed by counterstaining with eosin (Poly Scientific R&D Corp.) for 4 minutes. The immunohistochemistry was performed at the Molecular Cytology Core Facility of Memorial Sloan Kettering Cancer Center using MIRAX Slide Scanning System (PerkinElmer).

Statistical analysis

All *in vitro* experiments were carried out at least two to three times. For *in vitro* and *in vivo* studies, *P* values were calculated using a Student *t* test. We selected *P* values of ≤ 0.05 as being statistically significant. SE was calculated as the SD divided by the square root of the number of samples.

Results

c-Met expression and HGF secretion in uveal melanoma cells

We evaluated the expression of the c-Met receptor and its basal phosphorylation status in uveal melanoma cells grown in serum-free media for 24 hours (Fig. 1A). All uveal melanoma cell lines tested express the c-Met receptor, represented by a 170 kDa precursor and a 145 kDa mature receptor. Examination of the sum of the two bands indicates that the cell lines with G-protein mutations namely, 92.1, Omm1.3, and Omm1, expressed relatively more c-Met than the wild-type cell lines namely, C918, Mel290, and Mel285. Phospho-Met was also relatively higher in G-protein mutant cell lines than in wild-type cell lines, particularly in Omm1.3 cells, which had the most receptor phosphorylation. As the phosphorylation of c-Met is stimulated by the ligand, HGF, we investigated the ability of uveal melanoma

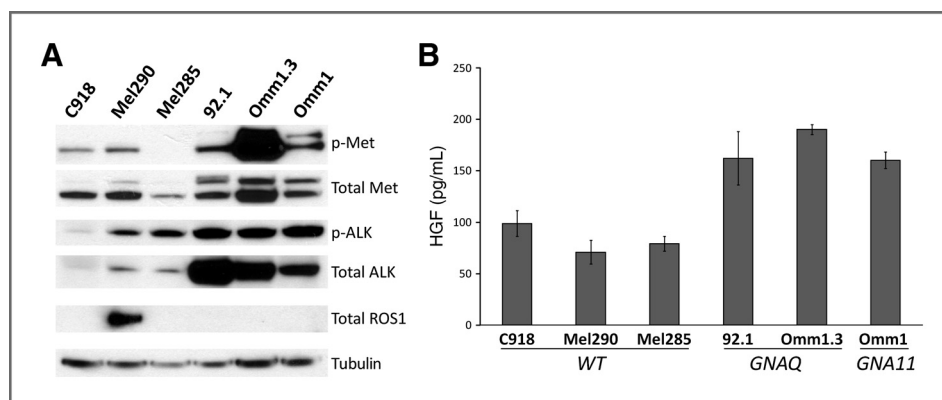


Figure 1. Expression of c-Met in uveal melanoma cells and HGF secretion. A, cells were grown in serum-free media for 24 hours and lysed for immunoblot analysis. c-Met expression and phosphorylation is generally higher in cell lines with G-protein mutations. B, media from the plates were tested for the presence of HGF by ELISA. All cell lines secreted HGF but the average HGF secretion of G-protein mutant cell lines was higher than the wild-type cell lines.

cells to secrete HGF in serum-free media using ELISA (Fig. 1B). After a 24-hour incubation period, cells released HGF ranging from 70 to 190 pg/mL. The cell lines with G-protein mutations, 92.1, Omm1.3, and Omm1, secreted more HGF than the wild-type cell lines, C918, Mel290 and Mel285, suggesting that uveal melanoma cell lines with G-protein mutation may be activating the c-Met phosphorylation through an autocrine signaling mechanism.

Suppression of c-Met by siRNA knockdown inhibits migration of uveal melanoma cells

Because dysregulated c-Met induces tumor growth, angiogenesis and metastasis, we tested the effects of c-Met downregulation on cell proliferation and migration of these uveal melanoma cell lines. Western blot analysis confirmed decreased levels of c-Met in all the cell lines transfected with c-Met siRNA (Fig. 2A and B). In cell viability assays, cell growth was not affected

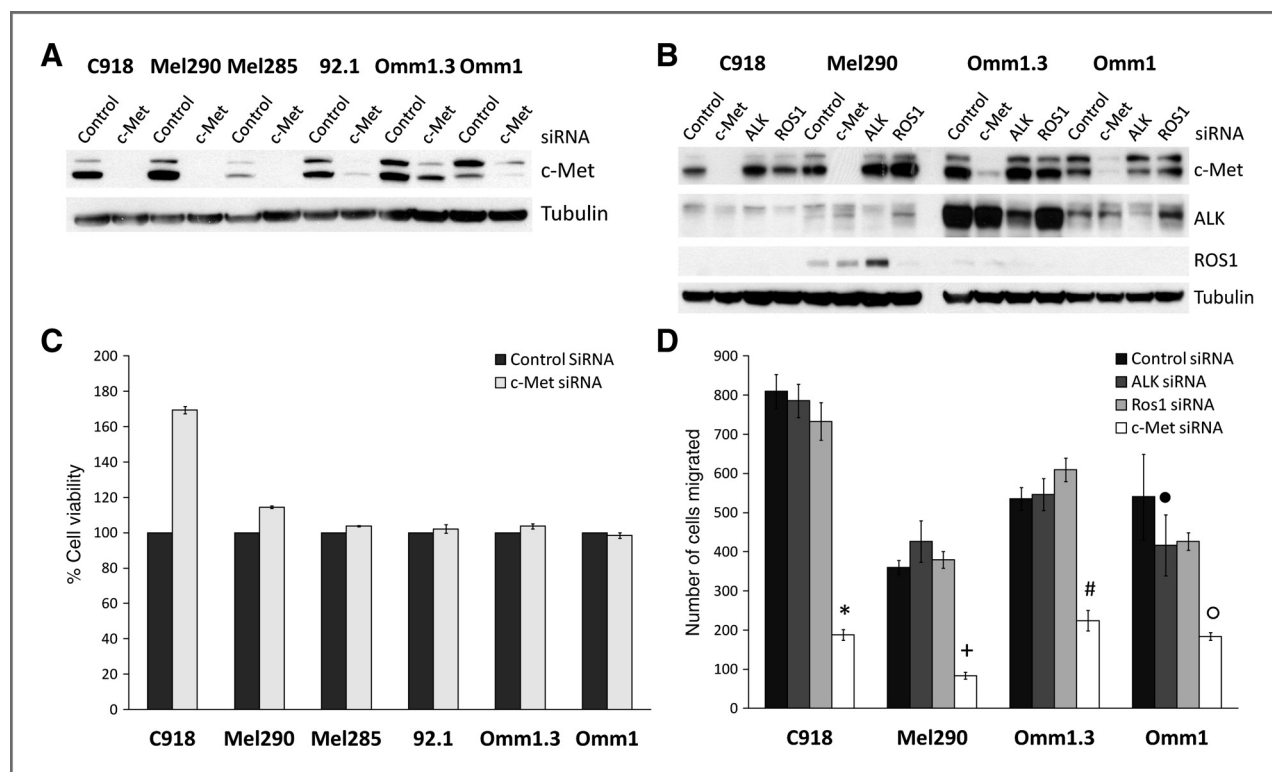


Figure 2. Effects of c-Met siRNA knockdown on cell proliferation and migration. A, uveal melanoma cells were transfected with control or c-Met siRNA. c-Met knockdown was verified by Western blot analysis of the lysates. B, cells were transfected with control, c-Met, ALK, or ROS1 siRNA. Western blot analysis of the lysates verified that all target genes were knocked down by their respective siRNA. C, transfected cells were plated in triplicates in 96-well plates and cell viability was measured after 72 hours as the percentage of control siRNA transfected cells. Knockdown of c-Met by siRNA does not affect the growth of uveal melanoma cell lines. D, transfected cells were seeded on Matrigel chambers in triplicates and allowed to migrate for 24 hours into RPMI media containing 10% serum. Migrated cells were then quantitated. Only c-Met siRNA knockdown inhibits cell migration (*, $P = 0.003$; +, $P = 0.002$; #, $P = 0.004$; °, $P = 0.039$). There was a decrease in migration of Omm1 cells transfected with ALK and ROS1 siRNA but it was not significant (*, $P > 0.05$).

by c-Met knockdown (Fig. 2C). On the other hand, c-Met siRNA significantly inhibited cell migration ($P < 0.05$; Fig. 2D and Supplementary Fig. S1) and this effect was independent of G-protein status. In view of the fact that crizotinib is also an inhibitor of ALK and ROS1 kinases, we used the siRNA knockdown strategy in suppressing ALK and ROS1 (Fig. 2B) to investigate whether these kinases have any effect in uveal melanoma migration. ALK and ROS1 knockdown did not significantly inhibit the migration of uveal melanoma cells (Fig. 2D and Supplementary Fig. S1). There was a slight decrease in migration of Omm1 cells transfected with ALK and ROS1 siRNA, but it was not statistically significant ($P > 0.05$). Collectively, these results indicate that cell migration of uveal melanoma cells is dependent on activated c-Met but not ALK or ROS1 and selectively suppressing c-Met decreases cell migration.

Crizotinib inhibits migration of uveal melanoma cell lines

We next elected to determine whether crizotinib would have a similar effect on cell migration. For these studies, we wanted to select the minimal concentration necessary to selectively inhibit p-Met but would have no effect on cell growth. The effects of crizotinib on the cell growth of uveal melanoma cell lines, wild-type or mutant for *GNAQ* and *GNA11*, were evaluated using a range of concentrations from 10 to 3,000 nmol/L (Fig. 3A). After 72 hours of treatment, all uveal melanoma cell lines showed a dose-dependent decrease in cell viability in response to crizotinib treatment. However, this effect only occurred at doses $\geq 1,000$ nmol/L. We found that c-Met phosphorylation was inhibited by crizotinib starting at 25 nmol/L, whereas neither ALK nor ROS1 was inhibited at any of the concentrations tested with 24 hours of drug exposure (Fig. 3B). In

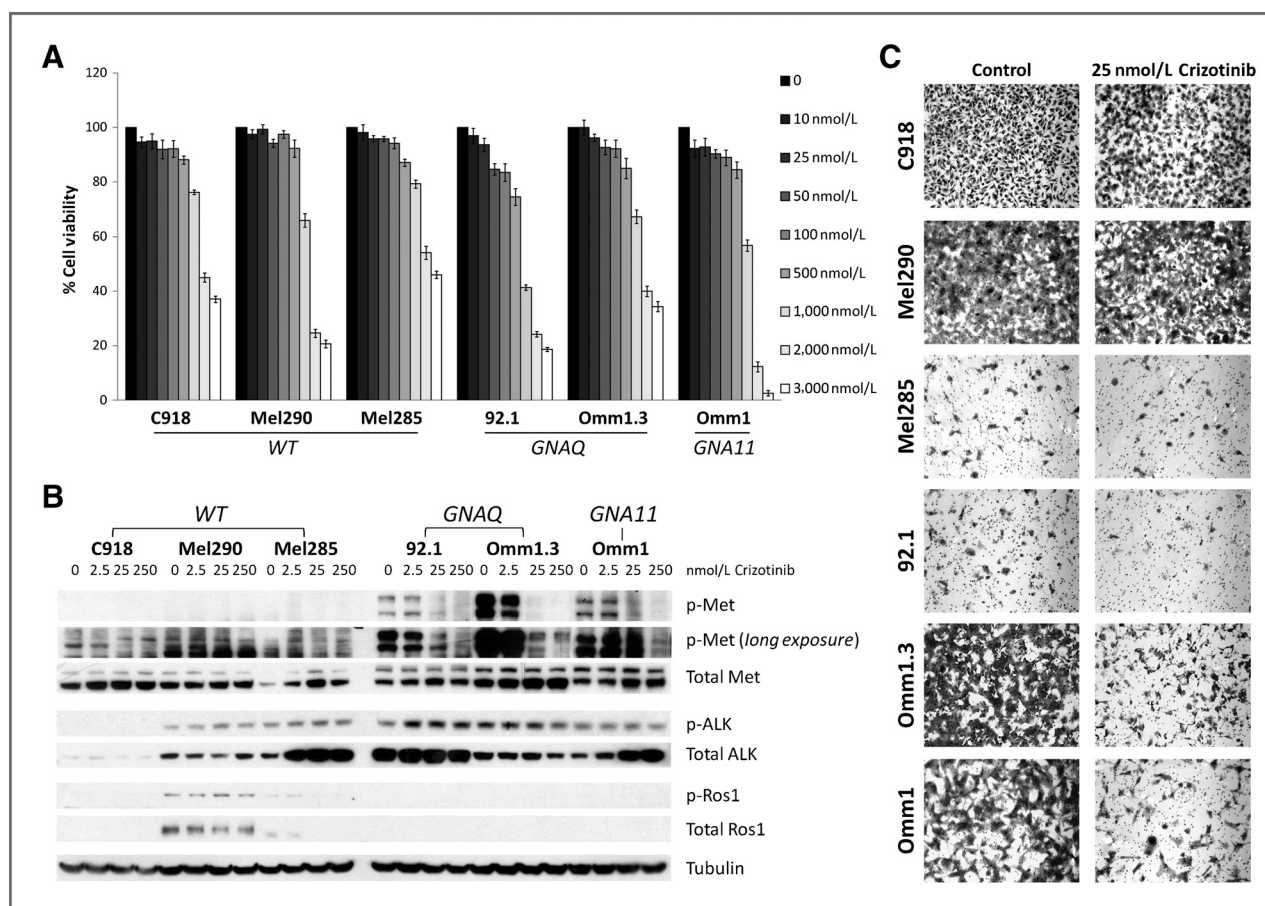


Figure 3. Effects of crizotinib on cell growth and cell migration. **A**, uveal melanoma cells were plated and treated in triplicates with increasing doses of crizotinib for 72 hours in 96-well plates then cell viability was measured as the percentage of untreated controls. Crizotinib inhibited cell proliferation in a dose-dependent manner regardless of genotype only at higher concentrations. The IC_{50} range is from 750 to 2,000 nmol/L. **B**, cells were grown to 60% confluency in 60-mm plates then treated with increasing doses of crizotinib for 24 hours. Cells were then harvested and lysed for immunoblot analysis. c-Met was inhibited by crizotinib starting at 25 nmol/L but not p-ALK and p-ROS1. **C**, uveal melanoma cells were seeded on a Matrigel chamber with 0.1% FBS in RPMI and either DMSO or 25 nmol/L crizotinib. Cells were then allowed to migrate for 24 hours into media containing 10% FBS and 50 ng/mL HGF. The migration of GNAQ-mutant uveal melanoma cells was significantly inhibited when treated with 25 nmol/L crizotinib but not the migration of wild-type cell lines.

view of this, we elected to test crizotinib at 25 nmol/L in a 24-hour migration assay. As shown in Fig. 3C, when uveal melanoma cells were treated with 25 nmol/L of crizotinib, a mutation-dependent effect was observed such that only the migration of G-protein mutant cell lines and not G-protein wild type cell lines (C918 and Mel290) was decreased. However, when treated with 250 nmol/L crizotinib for 24 hours (conditions under which cell proliferation was still not affected), the migration of all cell lines was inhibited irrespective of mutational status (Supplementary Fig. S2), suggesting that G-protein mutant cells with higher basal activity of c-Met (Figs. 1A and 3B) are sensitive to lower concentrations of the drug.

Crizotinib has marginal effects on tumor growth inhibition in uveal melanoma xenografts

To examine the effects of c-Met inhibition *in vivo*, we developed a subcutaneous xenograft model by particularly exploiting two uveal melanoma *GNAQ*-mutant cell lines, one (92.1 cell line; Fig. 4A) derived from a primary

tumor and the other (Omm1.3 cell line; Fig. 4B) derived from a metastatic tumor. The mice were treated with vehicle control or 50 mg/kg crizotinib orally five times a week for 3 weeks, the maximally tolerated dose in the mice. Comparison of average tumor volume between the control and treated groups show that there were very minimal effects on crizotinib-mediated inhibition of tumor growth from both the primary and the metastatic cell lines ($P > 0.05$). Therefore, we examined whether the drug inhibited its target kinases and the downstream signaling pathways (Fig. 4C). Although, the administration of this drug dose resulted in a complete inhibition of phosphorylation of c-Met, there was no inhibition in phosphorylation of the other target kinases, p-ALK, and p-ROS1. Importantly, the common downstream signaling components also seemed to be generally unaffected as determined by unchanged levels of p-AKT, p-ERK, and p-STAT3. There was a slight decrease in p-ERK1/2 in the Omm1.3 cells, though this could be due to a decrease in total ERK1/2 protein expression. The detection of human HGF expression in the tumor xenografts supports the

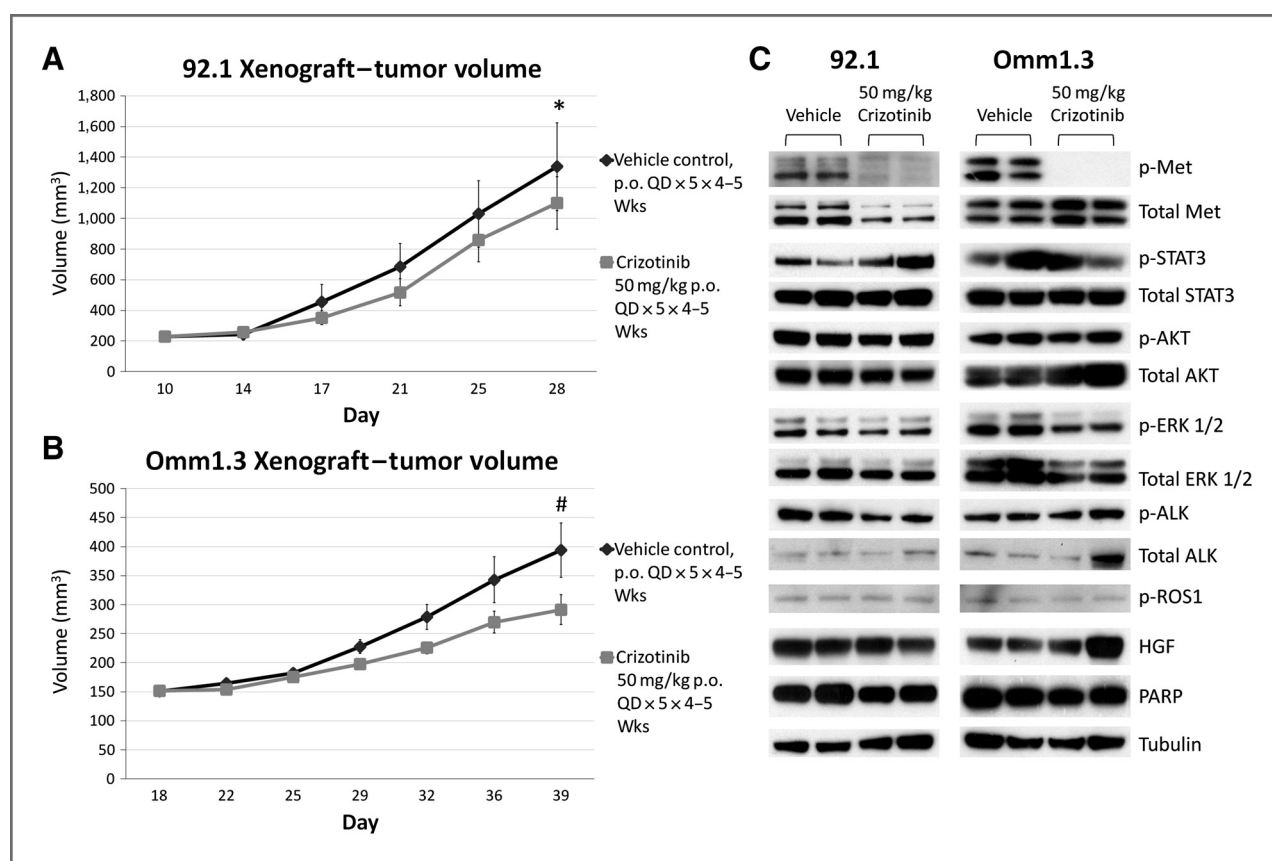


Figure 4. Tumor growth effects of inhibiting c-Met using crizotinib in uveal melanoma xenograft models. Eight-week-old nu/nu SCID male mice bearing subcutaneously injected 92.1 tumors (A) or Omm1.3 tumors (B) of approximately 100 mm³ diameter were treated orally with vehicle or 50 mg/kg/d crizotinib 5 days per week for 3 to 4 weeks (9 mice/cohort). There was no significant tumor growth inhibition by crizotinib. The P values were: *, $P = 0.47$; #, $P = 0.07$. C, of note, 92.1 and Omm1.3 tumors were collected from 2 mice per group. Protein lysates taken from frozen tumors were then immunoblotted to determine effects on c-Met signaling. Crizotinib completely inhibited p-Met *in vivo* with no inhibition of other drug targets and downstream kinases in both models.

hypothesis that HGF may activate c-Met through an autocrine activating loop in these cells. Apoptosis signaling at least via PARP cleavage was not observed in this study. There was no significant weight loss with this dose of crizotinib in either animal study (Supplementary Fig. S3A and S3B) and also attempts to increase the drug dose to 75 and 100 mg/kg, respectively, also showed no appreciable reduction in tumor volume though this was associated with some modest weight loss (Supplementary Fig. S4A and S4B).

Crizotinib prevents macrometastasis of uveal melanoma cells from developing *in vivo*

As there was only a minimal inhibition of tumor growth *in vivo* and that crizotinib inhibits migration *in vitro*, we next elected to determine whether crizotinib would prevent uveal melanoma metastasis *in vivo*. Therefore, we first developed a novel mouse model that represents a retro-orbital delivery of the uveal melanoma cells into circulation. The Omm1.3 cells were labeled with the EGFP-luciferase fusion protein. Thus, the labeled cells allowed us to verify the instant delivery of the transplanted cells and to monitor the mice for the subsequent development of metastatic disease by positron emission tomography imaging. To investigate the role of activated c-Met in these uveal melanoma cells, the mice were treated with 50 mg/kg crizotinib daily 5 days per week for 9 weeks starting from 7 days after the transplantation and were monitored weekly for the development of metastatic disease. Metastases were first observed 7 weeks later at which time most of the vehicle control mice showed strong luciferase activity in the eye, as well as at distant sites predominantly the liver and the lungs, whereas in crizotinib-treated mice, bioluminescence was predominantly seen at the site of primary transplantation (i.e., the eye; Fig. 5A). Luciferase activity was dramatically inhibited in the treated mice ($P = 0.03$), as determined by quantification of bioluminescence signal intensity (Fig. 5B). Necropsy images from representative vehicle-treated control animals show macroscopic tumors, substantiated by the bioluminescence in the livers, whereas there were no distinguishable tumors in the livers of crizotinib-treated mice (Fig. 5C). There was bioluminescence signal in the lungs of untreated animals, yet again there were no detectable bioluminescence signal in the lungs of treated animals. It is important to note that the uveal melanoma tumor growth in the eye of the mice was not inhibited by crizotinib. An H&E staining of liver sections from both cohorts verified the presence of metastatic tumor in the liver of untreated mice but not in the liver of crizotinib-treated mice (Fig. 5D). Two weeks after the end of drug treatment (i.e., on week 11), bioluminescence imaging showed continued tumor growth in the eye (the primary site), and in multiple distant sites, when compared with the mice treated with crizotinib (Supplementary Fig. S5A). In crizotinib-treated mice, metastases largely remained inhibited. Nec-

ropsy of the vehicle-treated mice revealed bioluminescence in the liver, lung, kidney, and spleen (Supplementary Fig. S5B). In addition, at week 11 the mice that previously responded to crizotinib now revealed small metastases in the liver.

Discussion

The development of macroscopically detectable metastasis occurs in 50% of patients with uveal melanoma, within 15 years of initial diagnosis, even after treatment and removal of the primary tumor (29). In our study, crizotinib inhibited c-Met phosphorylation and prevented uveal melanoma from forming macroscopic metastatic disease in a mouse model. We also observed a lack of antiproliferative effects by crizotinib at doses that selectively inhibit only c-Met. Interestingly, there was inhibition of cell growth *in vitro* at high concentrations of crizotinib but this can be attributed to potential off-target effects. There was also an observed increased expression of c-Met and ALK in Mel285 and Omm1 cells *in vitro* as well as in Omm1.3 tissues after treatment with crizotinib. This may be a potential survival mechanism but more studies are needed to evaluate the significance of this observation. In our xenograft model, there was only a minimal effect on tumor growth, which correlates with our *in vitro* study. Nevertheless, the xenograft studies do confirm inhibition of the target at the dose of drug administered. This is in contrast with past xenograft studies that have shown the potent antitumor activity of crizotinib in other tumor types (20–22). Other studies have found that the inhibition of c-Met alone may not be enough to prevent tumor growth *in vivo* and that other RTKs such as EGFR and IGF1R are critical for uveal melanoma cell survival (30, 31). In fact, inhibition of either phospho-Met or phospho-EGFR resulted in activation of alternative pathways and blockade of both receptors resulted in maximal inhibition of the downstream kinases p-AKT and p-ERK 1/2 (16, 30). Another study also demonstrated that combining inhibitors of c-Met and VEGFR slowed down tumor growth (17). Thus, c-Met inhibition with crizotinib alone seems insufficient in preventing uveal melanoma tumor growth *in vivo*. This ultimately may require the development of combination therapies with inhibitors of IGFR1, VEGFR, or EGFR.

In our *in vitro* studies, we found that a low nanomolar dose of crizotinib inhibited the migration of G-protein mutant cell lines but not wild-type cell lines. This may be explained by the higher basal levels of activated c-Met and secreted HGF, which possibly induces an autocrine response that activates the c-Met receptor, rendering the GNAQ and GNA11 mutant cells more sensitive to the drug than wild-type cells. However, when a higher dose of crizotinib is used, there is significant inhibition of cell migration in all uveal melanoma cells, an effect that is independent of G-protein mutational status. This effect can be recapitulated with siRNA specific to c-Met,

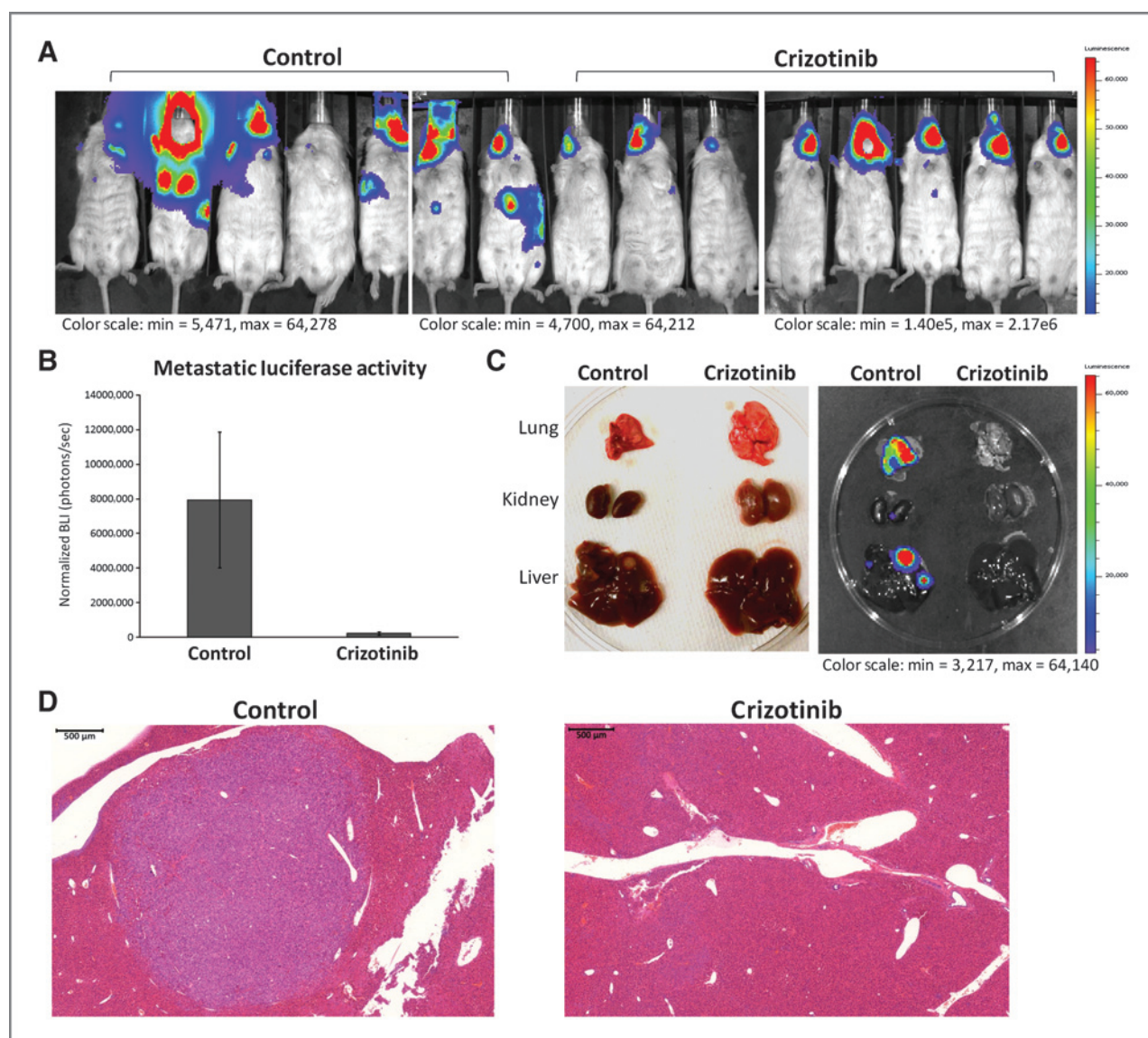


Figure 5. Inhibition of metastasis by crizotinib in a metastatic uveal melanoma model. Omm1.3 cells were stably infected with EGFP–luciferase and grown in large scale. The mice were then retro-orbitally injected with 10 million Omm1.3-EGFP–luciferase cells. One week after injection, the mice were treated with the vehicle or 50 mg/kg/d crizotinib 5 days a week for 9 weeks (10 control mice, 12 treated mice). The mice were imaged for luciferase activity every week. **A**, bioluminescence imaging at 7 weeks after injection of cells compared progression of metastasis in control- and crizotinib-treated mice. The control mice have metastasis in the abdominal region, whereas crizotinib inhibited metastasis in the treated mice. **B**, bioluminescence intensity was then quantified for each mouse and the mean calculated for each cohort. Luciferase activity in metastatic sites was significantly decreased in crizotinib-treated mice compared with the vehicle control ($P = 0.03$). **C**, necropsy images show macrometastases in the liver and lungs of the control mouse, whereas none were seen in the crizotinib-treated mouse. Bioluminescence imaging of the liver and lungs further illustrates inhibition of metastasis by crizotinib. **D**, H&E staining of liver tissue sections verify the presence of tumor in the control mouse liver but not in crizotinib-treated mouse liver.

which is not observed with siRNA for ALK or ROS1, the other targets of crizotinib. Previous studies have suggested the important role of c-Met overexpression in uveal melanoma metastasis and the regulation of its ligand, HGF, in determining tumor dissemination (32). Furthermore, c-Met–induced PI3K/AKT signaling has been linked to enhance cell migration of uveal melanomas (33). As we confirmed that c-Met plays a significant role in uveal melanoma cell migration, and that HGF is in fact expressed and secreted by these cells, a metastatic

model was developed to demonstrate the inhibition of metastasis by crizotinib.

Other studies have shown hepatic, bone, and visceral micrometastasis develop in a uveal melanoma xenograft model (34), as well as bone and visceral macrometastasis in an intracardiac metastatic mouse model (35). Another study has also demonstrated inhibition of micrometastasis using a VEGFR inhibitor after enucleation of the mouse eyes (36). In our study, we show that liver and lung metastases develop 6 to 7 weeks after retro-orbital

injection of EGFP-luciferase-infected uveal melanoma cells. We then demonstrated that crizotinib, at concentrations that inhibit p-Met *in vivo*, inhibited metastases from forming in the liver and lungs of the treated mice as compared with the control mice. We also observed that 2 weeks after stopping treatment with crizotinib, the mice previously treated with the drug showed traces of metastasis in the liver, but this was still significantly less than the control mice. The subsequent progression of metastasis after termination of treatment further illustrates the dependence of metastatic disease on c-Met signaling. It also illustrates that crizotinib is unable to kill the microscopic metastases that develop rapidly in both the liver and lungs after retro-orbital injection, but rather it seems to either prevent the cells from migrating or spreading to dominant visceral sites, especially the liver. This inability to eradicate small-volume disease ties in with the lack of single-agent efficacy observed in our *in vitro* and *in vivo* studies. The detection of circulating malignant cells capable of developing hepatic micrometastasis has also been reported at the time of the initial diagnosis of patients with primary uveal melanoma (37). These cells may become dormant and later reenter malignancy (38). It is conceivable that crizotinib is able to control these cells as long as the drug is maintained and then this inhibitory effect is lost once the drug is withdrawn, allowing metastatic lesions to develop.

Consistent with our *in vitro* and xenograft studies, we saw no inhibition of growth in the development of the eye lesions, even after the initiation of crizotinib therapy in the treated animals. Though this could be due to a lack of drug penetration into the orbit of the mouse, this is most likely consistent with our observation that inhibition of c-Met activity by crizotinib in uveal melanoma cells is in itself not sufficient to decrease tumor growth. Clinically, though, this is not a critical issue. Patients with primary uveal melanoma either have enucleation of the eye to remove the primary tumor or have plaque radiation to eradicate primary cancer cells at presentation.

Despite this approach, 50% of patients eventually develop metastatic disease and recurrence in the eye is exceptionally low (5, 6). The survival rate in patients with uveal melanoma decreases dramatically with the onset of metastasis (3, 4). Therefore, the critical issue remains how to prevent development of metastatic disease after the treatment of the primary tumor. These results suggest that it will be important to introduce preventive therapy as early as possible after initial presentation of this disease and that this therapy may need to be continued for the life time of the patient. There is now the potential to develop crizotinib as the first adjuvant therapy to prevent macrometastatic disease from developing in patients with uveal melanoma. Furthermore, with the metastatic uveal melanoma model we developed, more drugs can be screened to identify effective inhibitors against c-Met-dependent metastasis.

Disclosure of Potential Conflicts of Interest

No potential conflicts of interest were disclosed.

Authors' Contributions

Conception and design: O. Surriga, V.K. Rajasekhar, G.K. Schwartz
Development of methodology: O. Surriga, V.K. Rajasekhar, Y. Dogan, R. Huang, G.K. Schwartz
Acquisition of data (provided animals, acquired and managed patients, provided facilities, etc.): O. Surriga, R. Huang, G.K. Schwartz
Analysis and interpretation of data (e.g., statistical analysis, biostatistics, computational analysis): O. Surriga, R. Huang, G.K. Schwartz
Writing, review, and/or revision of the manuscript: O. Surriga, V.K. Rajasekhar, G. Ambrosini, R. Huang, G.K. Schwartz
Administrative, technical, or material support (i.e., reporting or organizing data, constructing databases): O. Surriga, G.K. Schwartz
Study supervision: G. Ambrosini, G.K. Schwartz

Grant Support

This study was supported by Cycle for Survival (Philanthropy; to O. Surriga, V.K. Rajasekhar, G. Ambrosini, and G.K. Schwartz).

The costs of publication of this article were defrayed in part by the payment of page charges. This article must therefore be hereby marked *advertisement* in accordance with 18 U.S.C. Section 1734 solely to indicate this fact.

Received June 20, 2013; revised October 9, 2013; accepted October 10, 2013; published OnlineFirst October 18, 2013.

References

- Shields CL, Kaliki S, Furuta M, Mashayekhi A, Shields JA. Clinical spectrum and prognosis of uveal melanoma based on age at presentation in 8,033 cases. *Retina* 2012;32:1363-72.
- Singh AD, Turell ME, Topham AK. Uveal melanoma: trends in incidence, treatment, and survival. *Ophthalmology* 2011;118:1881-5.
- Gragoudas ES, Egan KM, Seddon JM, Glynn RJ, Walsh SM, Finn SM, et al. Survival of patients with metastases from uveal melanoma. *Ophthalmology* 1991;98:383-9.
- Buzzacco DM, Abdel-Rahman MH, Park S, Davidorf F, Olencki T, Cebulla CM. Long-term survivors with metastatic uveal melanoma. *Open Ophthalmology J* 2012;6:49-53.
- Woodman SE. Metastatic uveal melanoma: biology and emerging treatments. *Cancer J* 2012;18:148-52.
- Bakalian S, Marshall JC, Logan P, Faingold D, Maloney S, Di Cesare S, et al. Molecular pathways mediating liver metastasis in patients with uveal melanoma. *Clin Cancer Res* 2008;14:951-6.
- Fournier GA, Albert DM, Arrigg CA, Cohen AM, Lamping KA, Seddon JM. Resection of solitary metastasis. Approach to palliative treatment of hepatic involvement with choroidal melanoma. *Arch Ophthalmol* 1984;102:80-83.
- Abdel-Rahman MH, Cebulla CM, Verma V, Christopher BN, Carson WE III, Olencki T, et al. Monosomy 3 status of uveal melanoma metastases is associated with rapidly progressive tumors and short survival. *Exp Eye Res* 2012;100:26-31.
- Harbour JW. The genetics of uveal melanoma: an emerging framework for targeted therapy. *Pigment Cell Melanoma Res* 2012;25:171-81.
- Harbour JW, Onken MD, Roberson ED, Duan S, Cao L, Worley LA, et al. Frequent mutation of BAP1 in metastasizing uveal melanomas. *Science* 2010;330:1410-3.
- Mallikarjuna K, Pushparaj V, Biswas J, Krishnakumar S. Expression of epidermal growth factor receptor, ezrin, hepatocyte growth factor, and c-Met in uveal melanoma: an immunohistochemical study. *Curr Eye Res* 2007;32:281-90.
- Liu X, Yao W, Newton RC, Scherle PA. Targeting the c-MET signaling pathway for cancer therapy. *Expert Opin Investig Drugs* 2008;17:997-1011.

13. Christensen JG, Burrows J, Salgia R. c-Met as a target for human cancer and characterization of inhibitors for therapeutic intervention. *Cancer Lett* 2005;225:1–26.
14. Furge KA, Zhang YW, Vande Woude GF. Met receptor tyrosine kinase: enhanced signaling through adapter proteins. *Oncogene* 2000;19:5582–9.
15. Day RM, Cioce V, Breckenridge D, Castagnino P, Bottaro DP. Differential signaling by alternative HGF isoforms through c-Met: activation of both MAP kinase and PI 3-kinase pathways is insufficient for mitogenesis. *Oncogene* 1999;18:3399–406.
16. Dulak AM, Gubish CT, Stabile LP, Henry C, Siegfried JM. HGF-independent potentiation of EGFR action by c-Met. *Oncogene* 2011;30:3625–35.
17. Sennino B, Ishiguro-Oonuma T, Wei Y, Naylor RM, Williamson CW, Bhagwandin V, et al. Suppression of tumor invasion and metastasis by concurrent inhibition of c-Met and VEGF signaling in pancreatic neuroendocrine tumors. *Cancer Discov* 2012;2:270–87.
18. Di Cesare S, Marshall JC, Logan P, Anteck E, Faingold D, Maloney SC, et al. Expression and migratory analysis of 5 human uveal melanoma cell lines for CXCL12, CXCL8, CXCL1, and HGF. *J Carcinogenesis* 2007;6:2.
19. Abdel-Rahman MH, Boru G, Massengill J, Salem MM, Davidorf FH. MET oncogene inhibition as a potential target of therapy for uveal melanomas. *Invest Ophthalmol Vis Sci* 2010;51:3333–9.
20. Christensen JG, Zou HY, Arango ME, Li Q, Lee JH, McDonnell SR, et al. Cytoreductive antitumor activity of PF-2341066, a novel inhibitor of anaplastic lymphoma kinase and c-Met, in experimental models of anaplastic large-cell lymphoma. *Mol Cancer Ther* 2007;6:3314–22.
21. Zou HY, Li Q, Lee JH, Arango ME, McDonnell SR, Yamazaki S, et al. An orally available small-molecule inhibitor of c-Met, PF-2341066, exhibits cytoreductive antitumor efficacy through antiproliferative, and antiangiogenic mechanisms. *Cancer Res* 2007;67:4408–17.
22. Yamazaki S, Skaptason J, Romero D, Lee JH, Zou HY, Christensen JG, et al. Pharmacokinetic–pharmacodynamic modeling of biomarker response and tumor growth inhibition to an orally available c-Met kinase inhibitor in human tumor xenograft mouse models. *Drug Metab Dispos* 2008;36:1267–74.
23. Daniels KJ, Boldt HC, Martin JA, Gardner LM, Meyer M, Folberg R. Expression of type VI collagen in uveal melanoma: its role in pattern formation and tumor progression. *Lab Invest* 1996;75:55–66.
24. Zuidervaart W, van Nieuwpoort F, Stark M, Dijkman R, Packer L, Borgstein AM, et al. Activation of the MAPK pathway is a common event in uveal melanomas although it rarely occurs through mutation of BRAF or RAS. *Br J Cancer* 2005;92:2032–38.
25. De Waard-Siebinga I, Blom DJR, Griffioen M, Schrier PI, Hoogendoorn E, Beverstock G, et al. Establishment and characterization of an uveal-melanoma cell line. *Int J Cancer* 1995;62:155–61.
26. Chen PW, Murray TG, Uno T, Salgaller ML, Reddy R, Ksander BR. Expression of MAGE genes in ocular melanoma during progression from primary to metastatic disease. *Clin Exp Metastasis* 1997;15:509–18.
27. Luyten GPM, Naus NC, Mooy CM, Hagemeyer A, Kan-Mitchell J, Van Drunen E, et al. Establishment and characterization of primary and metastatic uveal melanoma cell lines. *Int J Cancer* 1996;66:380–7.
28. Dogan Y, Ganser A, Scherr M, Eder M. Quantification of transforming capacity and cooperation of defined genetic alterations in myeloid malignancies. *Exp Hematol* 2010;38:11–9.
29. Kujala E, Mäkitie T, Kivelä T. Very long-term prognosis of patients with malignant uveal melanoma. *Invest Ophthalmol Vis Sci* 2003;44:4651–9.
30. Xu H, Stabile LP, Gubish CT, Gooding WE, Grandis JR, Siegfried JM. Dual blockade of EGFR and c-Met abrogates redundant signaling and proliferation in head and neck carcinoma cells. *Clin Cancer Res* 2011;17:4425–38.
31. Wu X, Zhou J, Rogers AM, Jänne PA, Benedettini E, Loda M, et al. c-Met, epidermal growth factor receptor, and insulin-like growth factor-1 receptor are important for growth in uveal melanoma and independently contribute to migration and metastatic potential. *Melanoma Res* 2012;22:123–32.
32. Hendrix MJ, Seftor EA, Seftor RE, Kirschmann DA, Gardner LM, Boldt HC, et al. Regulation of uveal melanoma interconverted phenotype by hepatocyte growth factor/scatter factor (HGF/SF). *Am J Pathol* 1998;152:855–63.
33. Ye M, Hu D, Tu L, Zhou X, Lu F, Wen B, et al. Involvement of PI3K/Akt signaling pathway in hepatocyte growth factor-induced migration of uveal melanoma cells. *Invest Ophthalmol Vis Sci* 2008;49:497–504.
34. Yang H, Fang G, Huang X, Yu J, Hsieh CL, Grossniklaus HE. *In vivo* xenograft murine human uveal melanoma model develops hepatic micrometastases. *Melanoma Res* 2008;18:95–103.
35. Nottling IC, Buijs JT, Que I, Mintardjo RE, van der Horst G, Karperien M, et al. Whole-body bioluminescent imaging of human uveal melanoma in a new mouse model of local tumor growth and metastasis. *Invest Ophthalmol Vis Sci* 2005;46:1581–7.
36. Yang H, Jager M, Grossniklaus HE. Bevacizumab suppression of establishment of micrometastases in experimental ocular melanoma. *Invest Ophthalmol Vis Sci* 2010;51:2835–942.
37. Callejo SA, Anteck E, Blanco PL, Edelstein C, Burnier MN Jr. Identification of circulating malignant cells and its correlation with prognostic factors and treatment in uveal melanoma. A prospective longitudinal study. *Eye* 2007;21:752–9.
38. Logan PT, Fernandes BF, Di Cesare S, Marshall JC, Maloney SC, Burnier MN Jr. Single-cell tumor dormancy model of uveal melanoma. *Clin Exp Metastasis* 2008;25:509–16.

Molecular Cancer Therapeutics

Crizotinib, a c-Met Inhibitor, Prevents Metastasis in a Metastatic Uveal Melanoma Model

Oliver Surriga, Vinagolu K. Rajasekhar, Grazia Ambrosini, et al.

Mol Cancer Ther 2013;12:2817-2826. Published OnlineFirst October 18, 2013.

Updated version Access the most recent version of this article at:
doi:[10.1158/1535-7163.MCT-13-0499](https://doi.org/10.1158/1535-7163.MCT-13-0499)

Supplementary Material Access the most recent supplemental material at:
<http://mct.aacrjournals.org/content/suppl/2013/10/17/1535-7163.MCT-13-0499.DC1>

Cited articles This article cites 38 articles, 12 of which you can access for free at:
<http://mct.aacrjournals.org/content/12/12/2817.full#ref-list-1>

Citing articles This article has been cited by 1 HighWire-hosted articles. Access the articles at:
<http://mct.aacrjournals.org/content/12/12/2817.full#related-urls>

E-mail alerts [Sign up to receive free email-alerts](#) related to this article or journal.

Reprints and Subscriptions To order reprints of this article or to subscribe to the journal, contact the AACR Publications Department at pubs@aacr.org.

Permissions To request permission to re-use all or part of this article, use this link
<http://mct.aacrjournals.org/content/12/12/2817>.
Click on "Request Permissions" which will take you to the Copyright Clearance Center's (CCC) Rightslink site.